Catena 196 (2021) 104827

Contents lists available at ScienceDirect

Catena

journal homepage: www.elsevier.com/locate/catena

Splash erosion affected by initial soil moisture and surface conditions under simulated rainfall

Nives Zambon[a,*], Lisbeth Lolk Johannsen[a], Peter Strauss[b], Tomas Dostal[c], David Zumr[c], Thomas A. Cochrane[d], Andreas Klik[a]

[a] University of Natural Resources and Life Sciences, Department of Water, Atmosphere & Environment, Vienna, Austria
[b] Institute for Land and Water Management Research, Petzenkirchen, Austria
[c] Czech Technical University in Prague, Faculty of Civil Engineering, Prague, Czech Republic
[d] University of Canterbury, Department of Civil and Natural Resources Engineering, Christchurch, New Zealand

ARTICLE INFO

Keywords:
Splash erosion
Rainfall kinetic energy
Rainfall simulator
Saturated hydraulic conductivity
Surface sealing
Ponding

ABSTRACT

Soil erosion by water is one of the most severe soil degradation processes. Splash erosion is the initial stage of soil erosion by water, resulting from the destructive force of rain drops acting on soil surface aggregates. Apart from rainfall properties, constant soil physical properties (texture and soil organic matter) are crucial in understanding the splash erosion. However, there is lack of information about the effect of variable soil properties such as soil initial water content and surface condition (seal formation) on splash erosion. The objective of the present study was to determine how initial water content and surface condition affected soil splash erosion under simulated rainfall. The changes in soil surface condition were characterized by hydraulic variability (saturated hydraulic conductivity) due to surface seal formation. Slit loam and loamy sand soil textures were used in the experiment. The soil samples were collected from the top layer; air dried, and filled into modified Morgan splash cups for splash erosion measurements. Rainfall was created in the laboratory using two types of rainfall simulators covering intensity range from 28 to 54 mm h^{-1} and from 35 to 81 mm h^{-1}. The soil samples were exposed to three consecutive rainfall simulations with different time intervals between simulations and different initial water content and surface conditions (air-dried, wet-sealed, and dry-crusted). Wet-sealed soil samples had up to 70% lower splash erosion rate compared to air-dried samples, due to surface ponding followed by seal formation. A significant decrease in soil saturated hydraulic conductivity indicated the formation of surface seal for silt loam soils. A non-significant decrease in saturated hydraulic conductivity for loamy sand soil was attributed to earlier formation of stable seals. Two different rainfall simulators produced different amount of splash erosion rates; however, the splash erosion development for increasing rainfall intensity was almost equal considering same initial surface condition. These results provide insight into dynamic changes of individual soil parameters affected by rainfall, and could find wider application for more complex soil erosion prediction models.

1. Introduction

Detachment of soil by rain drop impact is the first stage of the soil erosion process by water (Quansah, 1981). According to Rose (1960) and Hairsine and Rose (1991), splash has more influence on detached soil particles than surface runoff, before the stage of rill and gully erosion is reached. Bare soil surface exposed to rain drops changes its structural and hydraulic properties, which remarkably influences soil infiltration, soil water repellency, overland flow, and final soil erosion rates (Fernández-Raga et al., 2019). The main driver for the splash detachment process is the kinetic energy (KE) of rainfall, which depends on the amount, size, and fall velocities of the drops according to Wischmeier et al. (1971), Ghadiri and Payne (1977) and Morgan (2005). Together with rainfall characteristics, soil physical parameters are crucial in defining the soil erosion process. Wischmeier and Smith (1978) concluded that particle size distribution and organic matter content were the most dominant indicators of soil erodibility. Le Bissonnais (2016) also reported that soil mineralogy, soil texture, organic matter content and initial water content (θ_a) influence the formation of aggregates, where higher θ_a increases the resistance of aggregates against the rain drop impact.

At the beginning of rainfall, KE of rain drops has to exceed a

* Corresponding author at: Institute for Soil Physics and Rural Water Management (SoPhy), University of Natural Resources and Life Sciences (BOKU), Muthgasse 18, 1190 Vienna, Austria.
E-mail address: nives.zambon@boku.ac.at (N. Zambon).

https://doi.org/10.1016/j.catena.2020.104827
Received 12 December 2019; Received in revised form 29 July 2020; Accepted 3 August 2020

threshold, in order to induce destruction of soil aggregates (Kinnell, 2005). If detached soil particles are deposited on the soil surface, they can cause pore filling and clogging by wash-in of fine soil particles (Assouline, 2004; McIntyre, 1958). Soil infiltration rate is then reduced with incipient surface ponding. During ponding the soil surface is rapidly sealed and the crust formation is dependent on cumulative rainfall KE (Baumhardt et al., 1990). Development of seal on soil surface depends on the soil characteristics, being mostly common for soils with high silt content and low organic matter (Armenise et al., 2018). When observing the interaction of splash erosion and seal development, Cheng et al. (2008) discovered that the splash erosion fluctuations are related to surface crust development, where the final splash rates were lower for the soils suspected to surface sealing. Furthermore, several researches have investigated the effect of ponding on soil erosion. For instance, Gao et al. (2003) proved that shallow water layer can accelerate the rain drop impact force on soil erosion, until it reaches a critical depth when the soil detachability decreases. However, they did not consider surface seal formation during ponding phase. Proposed by Guy et al. (1987), the defined critical ponding depth on soil surface is rainfall dependent and equal to three drop diameter.

During the rainfall, soil hydraulic and structural properties define the soil erosion and runoff production. Different approaches have been developed to describe the water movement through the soil affected by surface sealing. Assouline and Mualem (1997) related the seal formation to increase in soil bulk density. Furthermore, in later study (Assouline and Mualem, 2002), they proved that the use of saturated hydraulic conductivity (K_s) for an infiltration model can sufficiently describe the heterogeneity in soil hydraulic properties.

Many experimental studies (e.g. Kinnell, 1982; Salles et al., 2001; Salles and Poesen, 2000; Sharma et al., 1991) have been dealing with rainfall properties controlling splash erosion. However, there is still scarce information in most of these studies about the influence of soil physical properties (moisture, texture, structure, infiltration capacity etc.) on splash erosion. Few authors (Beczek et al., 2019; Truman and Bradford, 1990; Vermang et al., 2009) investigated the effect of different soil moisture on splash erosion, however, different results reported could be contributed to particular conditions in the experiment. Variable results were mainly concerning the different preventing mode, soil organic carbon and clay content of soil samples (Vermang et al., 2009), which can affect the result interpretation. Furthermore, there is lack of studies relating splash erosion with sealing and crust formation and its influence on infiltration (Fernández-Raga et al., 2017).

The main aim of this study is to investigate the effect of different soil moisture content and surface condition (seal formation) on splash erosion for three soils under simulated rainfall. The changes on soil surface were related to changes in soil K_s. Consequently, second objective is to quantify the differences in soil K_s affected by different rainfall intensities and corresponding KE. According to the recent knowledge of authors, the influence of different rainfall characteristics produced by two rainfall simulators on splash erosion development has never been investigated within one study. Therefore, a third objective is to quantify the differences between rainfall characteristics produced by two rainfall simulators and their impact on soil splash erosion for different soil initial conditions.

2. Materials and methods

2.1. Soil sampling

Soil samples were taken from three different locations. Two locations, Zwerbach (15°14′46.09″E, 48° 8′21.91″N) and Mistelbach (16°35′16.07″E, 48°35′2.60″N), are located in agricultural parts of Lower Austria. Third location is situated in Býkovice (14°50′20.0″E, 49°45′41.5″N) within the Central Bohemian Region in Czech Republic. Further on, the soils from Mistelbach, Zwerbach and Býkovice will be referred as MI, ZW and BK, respectively. The samples were collected in spring 2017, after seed-bed preparation from the top soil layer (0–10 cm), air dried and sieved through 10 mm sieve. Particle size distribution was determined with a combined wet sieving and sedimentation method (ÖNORM L 1061-1; ÖNORM L 1061-2, 2002). Soil textures varied from silt loam to loamy sand (ÖNORM L 1050, 2016).[1] According to World Reference Base (WRB) classification (IUSS Working Group WRB, 2014) soils MI, ZW and BK are classified as Calcic Chernozem, Dystric Planosol and Dystirc Cambisoil, respectively.

Samples for chemical analyses were air-dried, crushed, mixed and passed through a 2 mm sieve. Total carbon content was analysed by dry combustion (ÖNORM L 1080, 2013, 2013) using a C/N Analyzer (Vario Max CN, Elementar). Soil organic carbon content (OC) was obtained by subtracting inorganic carbon content measured volumetrically by the Scheibler method with a Calcimeter (ÖNORM L 1084, 2016) from total carbon content measured by C/N Analyzer. Further, the calcium carbonate was measured with the calcimeter using the method by Scheibler (ÖNORM L 1084, 2016). Soil pH was determined in a 1:2.5 soil to water solution, using a glass electrode by Metrohm. Cation exchange capacity (CEC) was estimated by extraction of the effective exchangeable cations by barium chloride solution following ÖNORM L 1086-1, 2014. Aggregate stability (AS) of soils was determined with the wet sieving method according to Kemper and Koch (1966) in modified form. The physical and chemical properties of soils obtained from laboratory analysis are listed in Table 1.

2.2. Experimental design

The experiments took place at the Institute for Soil Physics and Rural Water Management at University of Natural Resources and Life Sciences in Vienna, Austria (BOKU) and the Institute of Land and Water Management Research in Petzenkirchen, Austria (BAW). Modified Morgan splash cups (Morgan, 1981) were used for the splash erosion measurements. The splash cups were constructed from PVC drainage pipe tops with the inner diameter of 10.5 cm (Fig. 1-a) and height of 5 cm (Fig. 1-b). In the bottom of the splash cup, holes were drilled, to ensure water drainage through the soil layer during the rainfall. First, two nylon meshes (500 and 1000 μm) were placed on the bottom of the splash cup, to prevent soil loss trough the holes (Fig. 1-a). Air-dried and sieved (aggregates $<$ 10 mm) soil material was filled into the splash cups. The soil was loosely packed in three layers to reach similar bulk density as in seedbed condition (1–1.2 g cm^{-3}) for each corresponding soil. Soil layers were levelled with a long metal needle. Top layer was filled up to 1 cm below the splash cup edge to prevent surface overflow during high intensities (Fig. 1-c). At the top layer soil aggregates were randomly distributed to achieve heterogeneous arrangement of the all fractions (from fine to coarse).

Splash cups were placed in the middle of a splash collector, with standing height of 30 cm and diameter of 45.5 cm (Fig. 1-d). Splash collector had an outlet, ensuring the drainage of rainfall water with detached soil into buckets placed underneath. After the exposure to rainfall, eroded soil was rinsed from the collector rim, filtered and oven dried at 105 °C. The splash weighted from the filters corresponds to splashed soil from the splash cup surface of 86.6 cm^2.

Fig. 2 illustrates schematic overview of experiments made with two rainfall simulators. The three soils (MI, ZW, BK) were subjected to three rainfall simulations of 30 min, with various rainfall intensities across the positions under the rainfall simulator and different initial soil surface conditions. The first rainfall simulation was performed on air-dried soil surface (AD, $\theta < 5\%$). Second rainfall simulation followed after 24 h on wet-sealed (WS, $\theta_a \sim 30\%$) and final (third) simulation on dry-

[1] Primary classifications of particle size distribution following ÖNORM L 1050, 2016 (1994): sand (particle sizes from 0.2 mm − 0.063 mm diameter), silt (particle sizes from 0.063 mm − 0.002 mm diameter), clay (particle sizes smaller than 0.002 mm).

Table 1
Physical and chemical properties of soil material (0–10 cm soil depth) including: particle size distribution, aggregate stability (AS), alkalescence (pH), calcium carbonate content ($CaCO_3$), organic carbon (OC) and cation exchange capacity (CEC).

Soil location	Sand [%]	Silt [%]	Clay [%]	Soiltexture	AS [%]	$CaCO_3$ [%]	pH	OC [%]	CEC [cMol/kg]
Mistelbach	11.2	70.4	18.4	Silt loam	18.3	10.3	7.7	1.6	26.2
Zwerbach	14.0	60.2	25.8	Silt loam	41.4	3.9	7.7	1.5	25.8
Býkovice	41.6	46.3	12.1	Loamy sand	63.3	< 0.92	7.2	1.7	20.7

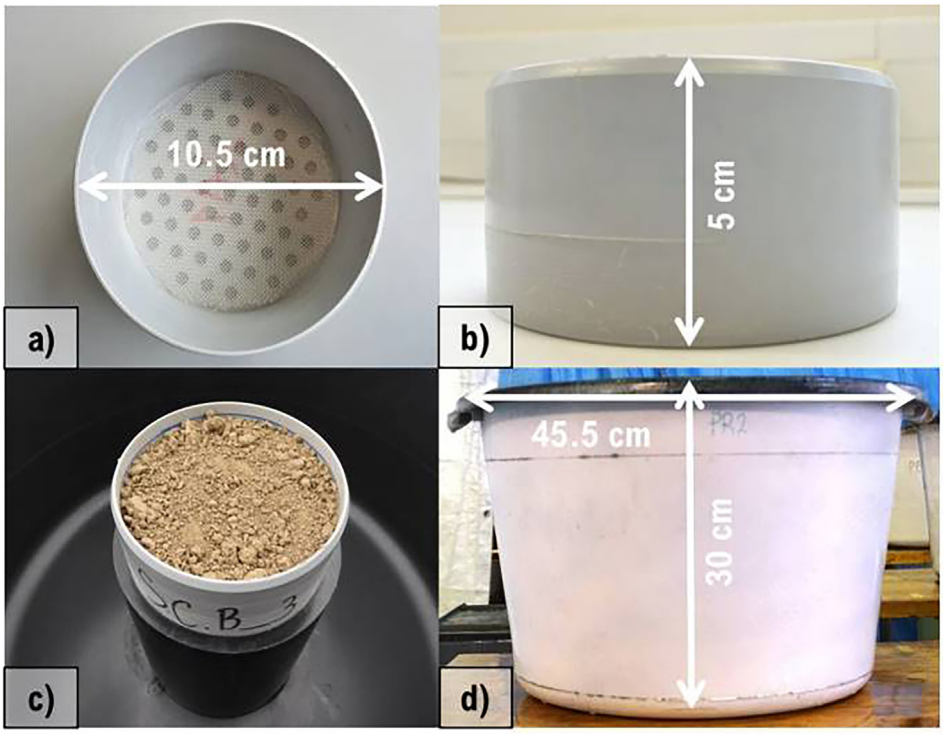

Fig. 1. Figure showing: (a) splash cup design from above; (b) splash cup design from side; (c) splash cup filled with soil and (d) splash collector design.

crusted soil surface (DC, 5% < θ_a < 10%) after approximately ten days of drying. A total of 9, 6 and 3 replications of splash erosion measurements were made for the AD, WS and DC surface condition, respectively. At the end of each rainfall simulation, K_s of soil samples was measured using constant head method, according to description by Klute and Dirksen (1987) at the BAW. Each measurement of soil K_s was replicated three times. Furthermore, the changes in soil infiltration rate were observed by measuring the time from the beginning of the rainfall until the appearance of surface ponding (accumulated water layer). This was defined as ponding time (t_p). Ponding was recorded by two cameras installed on the corners of experimental area under the BAW rainfall simulator. The cameras recorded a photo in one-minute interval during the rainfall simulation. Photos from the camera were analysed and the t_p was registered. Additionally, ponding was visually observed during the rainfall simulation where t_p for each soil sample was noted. The final t_p form camera and visual observation varied in ± 1 min, therefore t_p form the camera observations were taken as a reference.

Ponding was not temporary observed under the rainfall simulator at BOKU due to technical reasons; it was only noted if the samples had surface ponding or not after each experiment.

2.3. Rainfall simulators

For generating artificial rainfall two types of rainfall simulators were used. Norton Ladder type of rainfall simulator located at the BOKU consisted of four oscillating VeeJet 80100 spray nozzles, arranged in two rows and elevated 2.3 m above the splash cups. The simulated rainfall was operated with a pressure of 0.45 bar at the nozzles and the water was distributed from deionized water supply. Totally, nine different positions were arranged under the rainfall simulator for splash erosion measurements, as presented on the Fig. 3-a.

The rainfall simulator at BAW was equipped with one FullJet nozzle (½ HH-30WSQ), where intensity was controlled electronically by discontinuous spraying (Strauss et al., 2000). This design was deviating from normal use (three nozzles) to produce as much heterogeneity in rainfall intensity as possible. The nozzle was elevated 2.3 m above the splash cups and six positions were selected for splash erosion measurements (Fig. 3-b). The BAW rainfall simulator used deionized water with a constant water pressure of 0.25 bar at nozzles.

Rainfall simulations were performed for 30 min with a constant rainfall intensity rate. The maximum rainfall intensity tended to be between 40 and 80 mm h^{-1}, since it was attempted to keep the average intensity equal to those measured (data not shown) under natural rainfall at the locations from which the soil samples were collected. Real distribution of rainfall intensities below the simulators was measured for each position defined for splash erosion measurements, as shown on Fig. 3. Intensities were calculated from the accumulated water volume captured by the splash collectors and drained into the buckets beneath during 30 min rainfall simulation. Total volume of accumulated water in the buckets below the splash collectors was divided by the splash collector area (1625 cm^2). The intensities under the rainfall simulator at BOKU were measured after each experiment with soil samples. The mean of totally three replicates per soil type and initial condition for defined position was used in the results. Under the

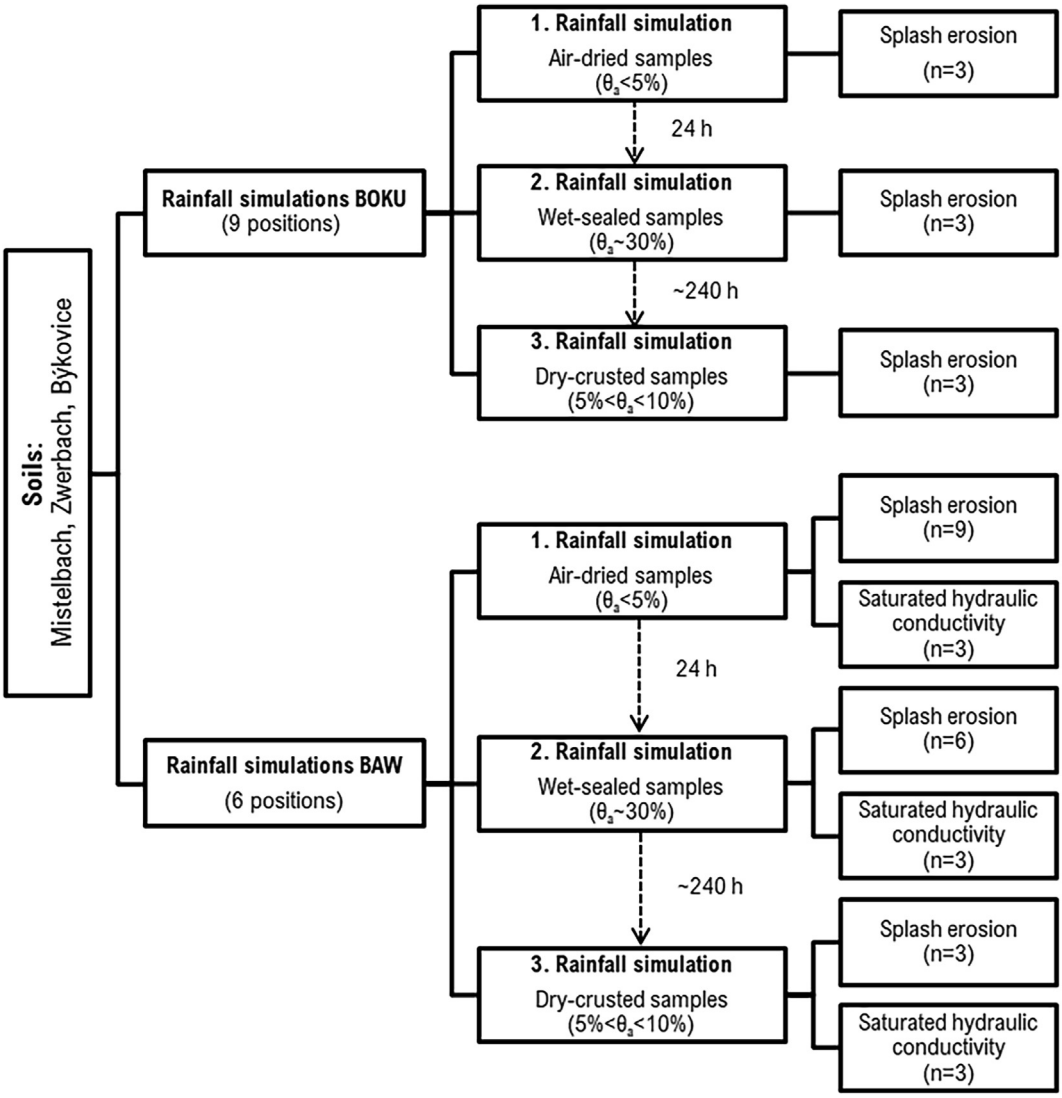

Fig. 2. Schematic overview of the splash erosion experiments for two rainfall simulators. The numbers in the parenthesis under splash erosion and saturated hydraulic conductivity indicate the number of replications per each soil. θ_a denotes the initial soil water content.

rainfall simulator at BAW, the intensity for defined positions of splash cups was calculated as the mean value obtained from totally six rainfall simulations (independent from soil or initial condition).

Rainfall KE, mean drop diameter, median drop diameter and mean drop fall velocity were derived from drop size distribution (DSD) measured with an optical laser disdrometer Weather Sensor OTT Parsivel Version 1 (Parsivel) by OTT Messtechnik. Parsivel disdrometer has a measuring area of 54 cm^2 and categorises the drops into 32 drop size and velocity classes (OTT, 2005). The KE under both rainfall simulators was obtained for each position defined for splash erosion measurements, as shown in Fig. 3. Disdrometer was centred on the positions of corresponding splash cups, which were previously marked on the ground. It was ensured that the height of the disdrometer laser beam is equal to the height of soil surface in the splash cup. For each position 15 min of rainfall was measured with the disdrometer.

The kinetic energy $KE_{i,j}$ (J m^{-2}) of rainfall per minute was computed for the diameter class i and velocity class j, that are provided by disdrometer, as follows:

$$KE_{i,j} = \frac{1}{2} m_i v_j^2 = \sum N \bullet \frac{1}{12 \bullet A} \bullet \pi \rho_w \bullet 10^{-6} \bullet D_i^3 \bullet v_j^2 \quad (1)$$

where m_i is the mean mass [g] corresponding to the drop diameter class i; N is number of detected raindrops of a certain size class i and velocity class j; A is the is the sampling area of the disdrometer (m^2); ρ_w is density of water (g cm^{-3}); D_i is mean drop diameter (mm) of size class i; and v_j is mean fall velocity (m s^{-1}) of velocity class j. The mass of raindrop was calculated assuming a spherical drop shape. Total KE is the sum of KEs for each drop size and velocity, multiplied with number of drops in the corresponding classes.

2.4. Statistical analysis

Statistical analyses were performed in R Studio (R Development Core Team, 2015). The Kruskal and Wallis (1952) test (one-way ANOVA on ranks) was used to identify statistical differences in K_s for different intensity rates (positions). Each position under the rainfall simulator represented one group of data for which the K_s was obtained. The positions (groups) differ in intensity rates which they are exposed to. The comparison is based on three replicates (n = 3) of K_s values obtained for each group (intensities). Multiple comparison between groups (post hoc) was further conducted with Dunn's test (Dunn, 1964) with *p*-adjustments of Benjamini-Hochberg (Benjamini and Hochberg, 1995). The differences in splash erosion rates between the three soils were analysed using the Student's *t*-test.

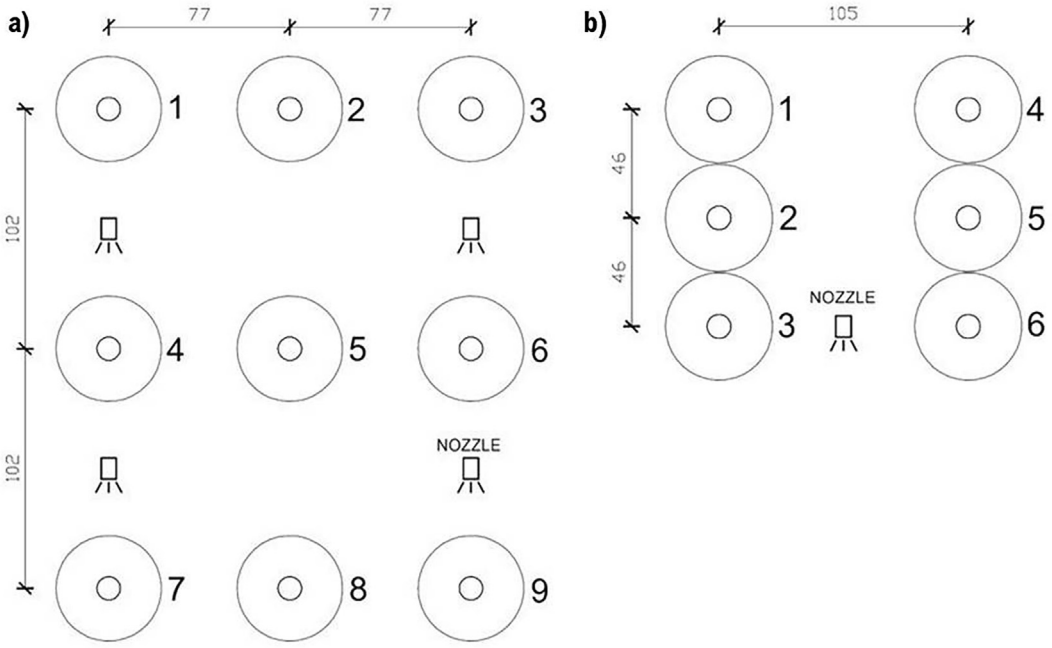

Fig. 3. Schematic representation of splash collectors (outer circle) and splash cup (inner circle) under positions marked for rainfall simulator at (a) BOKU and (b) BAW.

3. Results

3.1. Intensity and kinetic energy

According to intensity measurements, the rainfall simulators at BOKU and BAW covered intensity range from 28.2 to 54.2 mm h^{-1} (Table 2) and 35.3 to 81.2 mm h^{-1} (Table 3), respectively. Drop size distribution indicated that the rainfall simulator at BAW produced higher percentage of drops with drop diameter larger than 0.6 mm (Fig. 4-a), however, rainfall simulator at the BOKU had higher percentage of drops with velocity greater than 5.2 mm s^{-1} (Fig. 4-b). This resulted in larger mean and median drop size obtained for positions under the BAW rainfall simulator (Table 2) and higher mean raindrop velocity for positions under the BOKU rainfall simulator (Table 3). Distribution of mean drop velocity per drop size class (Fig. 5), indicated that 14% of total drops with diameter larger than 1.3 mm under the BAW rainfall simulator did not reach their terminal velocity, as specified by Atlas et al. (1973). Since the rainfall simulator at the BOKU produced higher velocity of larger drops, the resulting KE per mm of rainfall was on average 62% higher (Table 2) compared to KE per mm of rainfall for rainfall simulator at the BAW (Table 3). Total KE ranged between 504.4 and 923.1 J m^{-2} h^{-1} for the BOKU rainfall simulator (Table 2), and between 375.8 and 961.8 J m^{-2} h^{-1} for the BAW rainfall simulator (Table 3).

3.2. Splash erosion

Due to higher KE per mm of rainfall measured under the rainfall simulator at the BOKU, overall splash erosion rates were almost twice as high compared to results obtained with BAW simulator as shown on Fig. 6 (excluding the ZW soil for AD condition on Fig. 6-d).

For the rainfall simulator at BOKU, the MI soil had widest range of splash rates (0.06–0.58 kg m^{-2} h^{-1}) compared to ZW (0.02–0.31 kg m^{-2} h^{-1}) and BK (0.12–0.43 kg m^{-2} h^{-1}) soil. Splash erosion under the BAW rainfall simulator ranged similarly between three soils (0.02–0.23 kg m^{-2} h^{-1}) for AD initial condition (Fig. 6-a,d,g). The highest splash erosion was measured for samples exposed to KE of 667 J m^{-2} h^{-1} with largest drop diameter (Table 3). Relationship between splash erosion for three soils and KE was linear for the BOKU rainfall simulator, and non-linear for the BAW rainfall simulator (Table 4). Highest coefficient of determination (R^2) was calculated for ZW soil, considering both rainfall simulators. Between 60 and 72% less splash erosion, compared to simulation with AD initial condition, was measured for three soils with WS initial condition under both rainfall simulators. This reduction was evident for samples exposed to KE > 660 J m^{-2} h^{-1}, which were affected by surface ponding. However,

Table 2
Rainfall properties measured with collectors (intensity) and optical laser disdrometer under rainfall simulator at BOKU.

Position	Intensity [mm h^{-1}]	Kinetic energy [J m^{-2} h^{-1}]	Mean drop diameter* [mm]	Median drop diameter [mm]	Mean drop velocity** [m s^{-1}]	Kinetic energy/intensity [J m^{-2} mm^{-1}]
1	28.3	504.4	0.7	0.5	4.2	17.8
2	37.8	619.0	0.7	0.6	4.3	16.4
3	35.3	681.0	0.7	0.5	4.4	19.3
4	42.5	701.0	0.8	0.6	4.4	16.5
5	49.6	716.5	0.8	0.7	4.4	14.4
6	54.2	923.1	0.8	0.6	4.4	17.0
7	28.2	566.3	0.7	0.5	4.3	20.0
8	32.3	546.3	0.7	0.6	4.3	16.9
9	35.9	712.2	0.7	0.5	4.4	19.8

* The standard deviations of mean drop diameter were < 0.1 mm.
** The standard deviations of mean drop diameter were < 0.1 m s^{-1}.

Table 3
Rainfall properties measured with collectors (intensity) and optical laser disdrometer under rainfall simulator at BAW.

Position	Intensity [mm h^{-1}]	Kinetic energy [J m^{-2} h^{-1}]	Mean drop diameter [mm]	Median drop diameter* [mm]	Mean drop velocity** [m s^{-1}]	Kinetic energy/intensity [J m^{-2} mm^{-1}]
1	70.2	773.6	0.8	0.7	4.1	11.0
2	81.2	961.8	1.0	0.8	4.2	11.8
3	56.7	667.0	1.3	1.0	4.3	11.8
4	35.3	375.8	1.2	1.0	4.3	10.6
5	43.5	421.2	0.8	0.8	4.1	9.7
6	56.3	560.7	0.7	0.6	4.0	10.0

* The standard deviations of mean drop diameter were < 0.1 mm.
** The standard deviations of mean drop diameter were < 0.1 m s^{-1}.

splash erosion increased for samples exposed to lower KE. This was particularly noted for MI and ZW soil under the BOKU rainfall simulator (Fig. 6-b,e). Reduction in splash erosion for WS initial condition resulted in negative linear function between splash and KE with low R^2 (mostly < 0.10) considering both rainfall simulators (Table 4). The splash erosion for the samples with DC surface condition increased with KE, except for BK soil under the BOKU rainfall simulator (Fig. 6-i). Similarly to splash erosion results with WS condition, MI and ZW soil showed increase of roughly 50% in splash erosion rates for the samples exposed KE < 660 J m^{-2} h^{-1} (Fig. 6-c,f). Highest R^2 between splash erosion for three soils and KE was obtained for samples under the BAW rainfall simulator (Table 4).

3.3. Saturated hydraulic conductivity

Splash erosion affected by surface ponding during the rainfall simulations was contributed to different θ_a and changes in soil hydraulic properties. To quantify this changes soil K_s was measured after each rainfall simulation with different soil initial condition. Fig. 7 represents average K_s (n = 3) for the three soils and three initial conditions. Highest K_s between three soils were measured for ZW soil with the maximum of 1,102.9 mm h^{-1} obtained for initial AD surface condition (Fig. 7-d). Lowest values were measured for DC surface condition (Fig. 7-f). Similar trend was observed for MI soil, where highest K_s of 461.7 mm h^{-1} decreased to 56.3 mm h^{-1} for DC surface condition (Fig. 7-a,c). Generally, BK soil exhibited lowest K_s between three soils with maximum K_s of 193 mm h^{-1} for WS initial surface condition (Fig. 7-g-i). When comparing the K_s values measured for individual surface conditions it was observed that the samples exposed to lower (< 56.7 mm h^{-1}) intensities had higher K_s than samples exposed to high intensities. These differences were significant ($P < 0.05$) for MI soil with AD samples (Fig. 7-a), including ZW soil with WS and DC samples (Fig. 7-e,f). Furthermore, high variations between the replicates, typical for the samples exposed to lower intensities (< 56.7 mm h^{-1}), could result in no significant ($P > 0.05$) difference between K_s obtained for AD and WS surface condition considering three soils (Fig. 7-b,d,h).

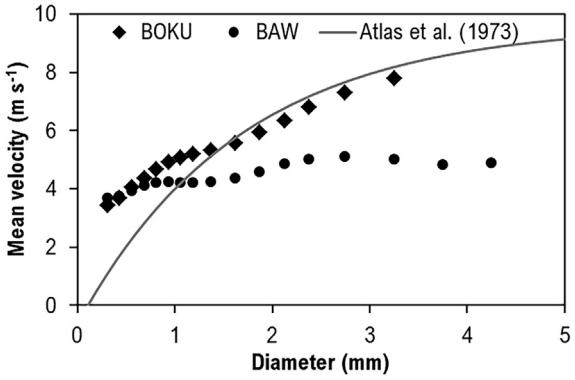

Fig. 5. Mean drop velocity of each drop size class for all positions measured under rainfall simulator at BAW and BOKU and terminal fall velocity line drawn according to Atlas et al. (1973). The velocities are shown for drop size classes within the total drops amount was larger than 100.

3.4. Relationship between soil saturated hydraulic conductivity and rainfall kinetic energy

As shown in previous results, the K_s of soil samples tend to decrease with the increasing intensity and after subsequent exposure to rainfall. To investigate the impact of KE on K_s, total KE applied on soil surface during the three rainfall simulations was plotted against K_s measured for each soil initial condition (Fig. 8). The relationship obtained for MI, ZW and BK soil can be described as a power function of accumulated KE, which agrees best for MI and ZW soil with R^2 of 0.54 and 0.74, respectively, where for BK soil low R^2 of 0.22 was obtained.

From the KE-K_s functions obtained, the decrease in K_s with increasing KE was observed until reaching a steady state, where KE had no impact on further K_s reduction. Assuming that the decrease in K_s was accompanied with a surface sealing, constant K_s values would indicate a final stage in the surface seal formation. The amount of KE needed for fully developed surface sealing could be calculated by considering the impact of KE on soil K_s. After a certain amount of KE applied on the soil

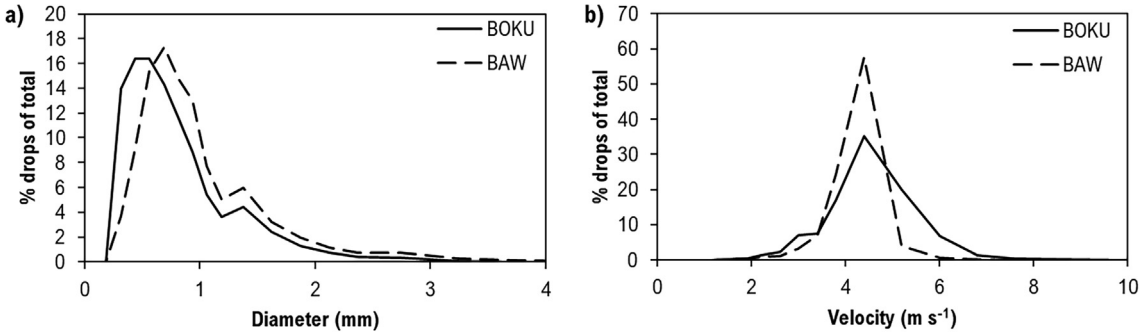

Fig. 4. Mean drop size and velocity distribution including all positions under rainfall simulator at BOKU and BAW. Each drop size and velocity class is percentage of drops within the class out of the total drops amount (classes with < 100 drops were not considered).

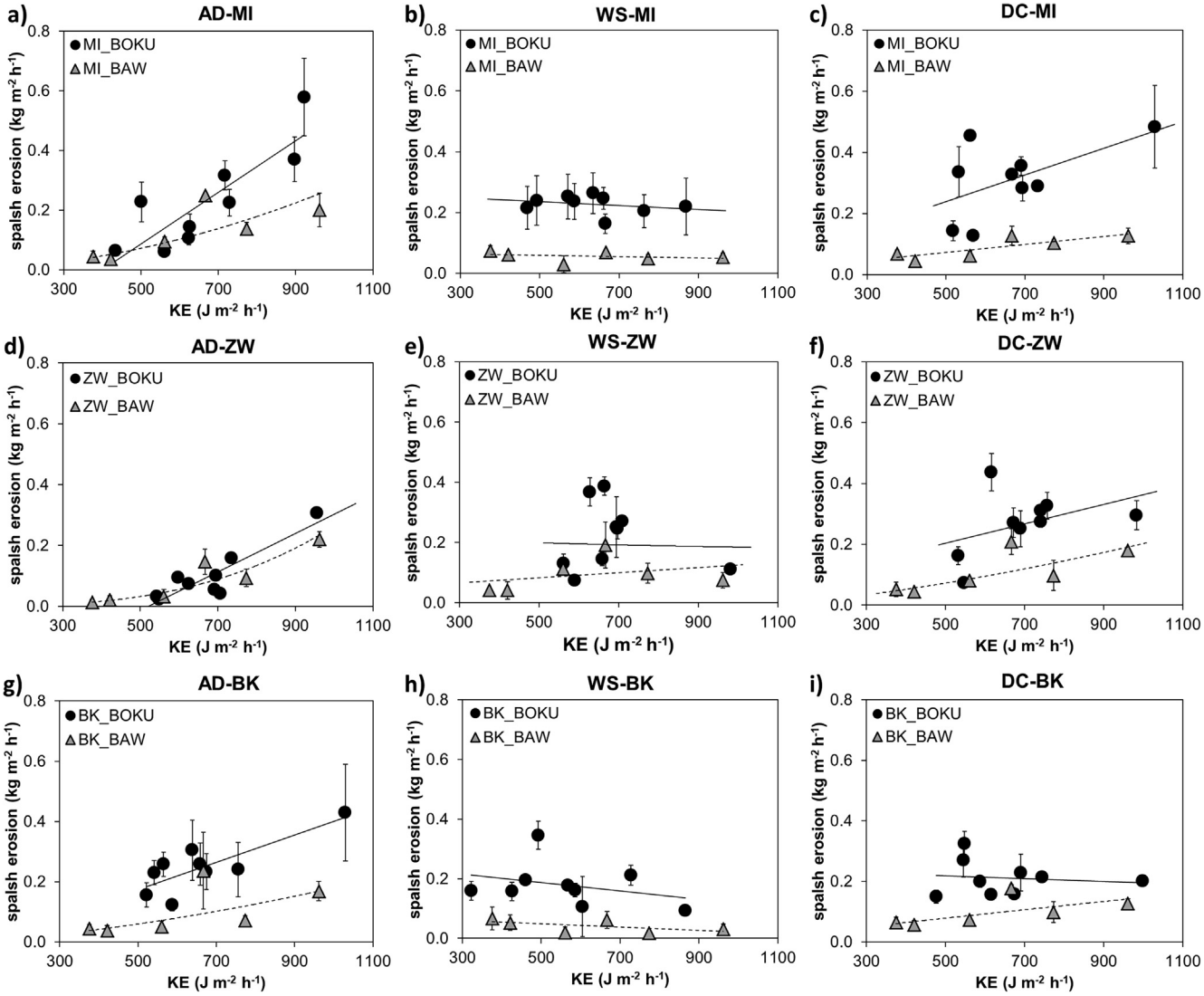

Fig. 6. Mean splash erosion plotted against rainfall kinetic energy (KE) obtained under rainfall simulator at BOKU and BAW. Splash erosion is shown for: (a-c) Mistelbach (MI), (d-f) Zwerbach (ZW) and (g-i) Býkovice (BK) soil with respect to air-dried (AD), wet-sealed (WS) and dry-crusted (DC) surface initial condition. Whiskers indicate ± standard deviation of mean splash erosion within replicates (n = 3, 6, 9).

Table 4
Linear and nonlinear regression with associated determination coefficient (R^2) between kinetic energy (KE) (kJ m^{-2} h^{-1}) and splash erosion (S) (kg m^{-2} h^{-1}) obtained for two rainfall simulators, at BOKU and BAW institute, and Mistelbach (MI), Zwerbach (ZW) and Býkovice (BK) soil with air-dried (AD), wet-sealed (WS) and dry-crusted (DC) soil initial condition (IC).

Soil	IC	BOKU	R^2	BAW	R^2
MI	AD	S = 9E-04 KE − 0.35	0.73	S = 5E-07 KE ^ 1.92	0.77
ZW	AD	S = 6E-04 KE − 0.33	0.80	S = 2E-10 KE ^ 3.02	0.90
BK	AD	S = 5E-04 KE − 0.05	0.65	S = 3E-06 KE ^ 1.59	0.56
MI	WS	S = -6E-05 KE + 0.27	< 0.10	S = -2E-05 KE + 0.07	< 0.10
ZW	WS	S = -1E-04 KE + 0.31	< 0.10	S = 9E-05 KE + 0.04	0.11
BK	WS	S = -1E-04 KE + 0.25	< 0.10	S = -6E-05 KE + 0.08	0.32
MI	DC	S = 4E-04 KE − 0.02	0.32	S = 1E-04 KE + 0.07	0.68
ZW	DC	S = 3E-04 KE − 0.04	0.18	S = 7E-06 KE ^ 1.48	0.70
BK	DC	S = -5E-05 KE + 0.24	< 0.10	S = 3E-03 KE ^ 0.90	0.56

surface, K_s significantly ($P < 0.05$) varied for increasing KE until reaching a constant value (Fig. 8). This amount of KE was addressed as the threshold value required for fully developed seal formation and it represented the transformation point between variable and constant soil K_s. Accordingly, the calculated threshold value of accumulated kinetic energy (KE_0) was found to be 0.39 kJ m^{-2} for MI soil and 0.59 kJ m^{-2} for ZW soil (Fig. 8-a,b). The BK soil showed no significant impact of increasing KE on K_s; therefore, the threshold value could not be obtained (Fig. 8-c).

3.5. Surface ponding

Present surface ponding was mostly concentrated within samples in central positons under the rainfall simulator at BOKU (e.g. positon 2, 4, 5, 6, and 8), where the drops overlapped (Table 2). For these positons higher KE and lower final splash erosion rates were measured, compared to positons with no surface ponding. During the rainfall simulation at the BAW, t_p was recorded for each soil sample in splash cup (Table 5). Generally, highest t_p was measured for the AD and DC surface condition, and lowest for WS surface condition. This was expected considering that samples with AD and DC initial condition had higher infiltration capacity due to lower θ_a and samples with WS initial condition had lower infiltration capacity due to higher θ_a. Furthermore, this results correlated to the K_s values obtained for the three soils. The shortest t_p was measured for BK soil, which had the lowest K_s and longest t_p for the ZW soil with highest K_s compared to other soils.

Measured t_p for the samples with WS initial condition was related to

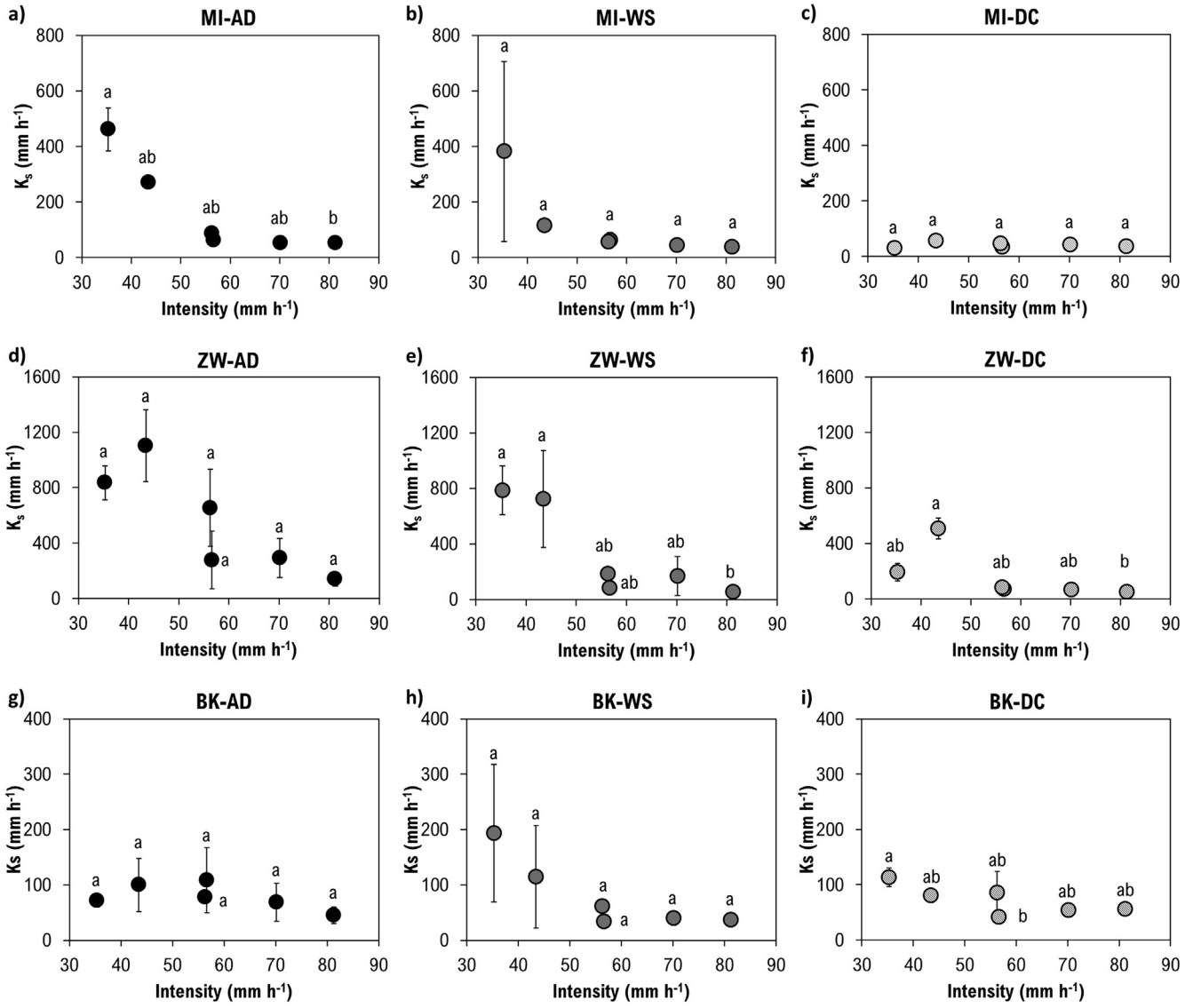

Fig. 7. Mean soil saturated hydraulic conductivity (K_s) obtained for (a-b) Mistelbach (MI), (d-f) Zwerbach (ZW) and (g-i) Býkovice (BK) soil with (AD), wet-sealed (WS), and dry-crusted (DC) surface initial condition. Letters indicate difference at significance level $P < 0.05$ between Ks obtained for different intensity rates under BAW rainfall simulator. Whiskers indicate ± standard deviation of the mean K_s within replicates (n = 3).

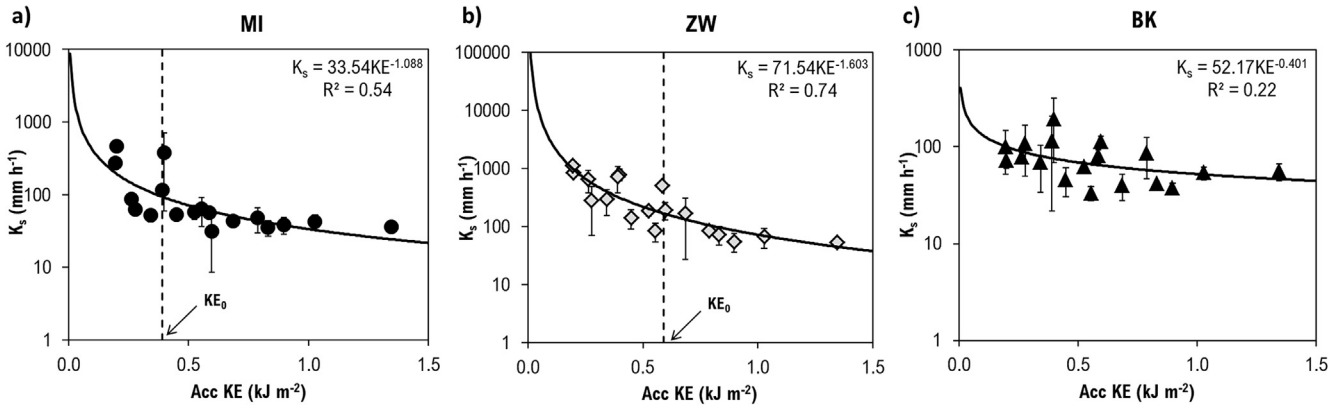

Fig. 8. Regression analysis of mean soil saturated hydraulic conductivity (K_s) in logarithmic scale plotted against accumulated rainfall kinetic energy (Acc KE) for: (a) Mistelbach (MI), (b) Zwerbach (ZW) and (c) Býkovice (BK) soil. The dashed line shows the threshold (KE_0) separating the variable from constant K_s values. Whiskers represent ± standard deviation of mean K_s within replicates (n = 3).

Table 5
Average time to ponding (t_p) (± standard deviation) from three observations (n = 3) during rainfall simulation with Mistelbach (MI), Zwerbach (ZW) and Býkovice (BK) soil obtained for three different soil initial conditions: air-dried (AD), wet-sealed (WS) and dry-crusted (DC). Positons with soil samples where no ponding was detected are marked as (−) under the column t_p.

Soil	Position	Intensity [mm h^{-1}]	t_p AD [min]	t_p WS [min]	t_p DC [min]
MI	1	70.2	21 (± 0)	6 (± 1)	17 (± 3)
MI	2	81.2	20 (± 2)	4 (± 0)	10 (± 3)
MI	3	56.7	23 (± 0)	6 (± 0)	18 (± 2)
MI	4	35.3	–	27 (± 0)	–
MI	5	43.5	–	11 (± 0)	–
MI	6	56.3	–	8 (± 2)	28 (± 1)
ZW	1	70.2	–	10 (± 2)	24 (± 0)
ZW	2	81.2	–	6 (± 2)	22 (± 2)
ZW	3	56.7	–	8 (± 2)	–
ZW	4	35.3	–	–	–
ZW	5	43.5	–	–	–
ZW	6	56.3	–	25 (± 0)	–
BK	1	70.2	24 (± 2)	4 (± 0)	18 (± 1)
BK	2	81.2	18 (± 3)	3 (± 0)	10 (± 0)
BK	3	56.7	21 (± 1)	4 (± 0)	20 (± 0)
BK	4	35.3	–	–	–
BK	5	43.5	–	11 (± 5)	–
BK	6	56.3	20 (± 0)	7 (± 0)	21 (± 3)

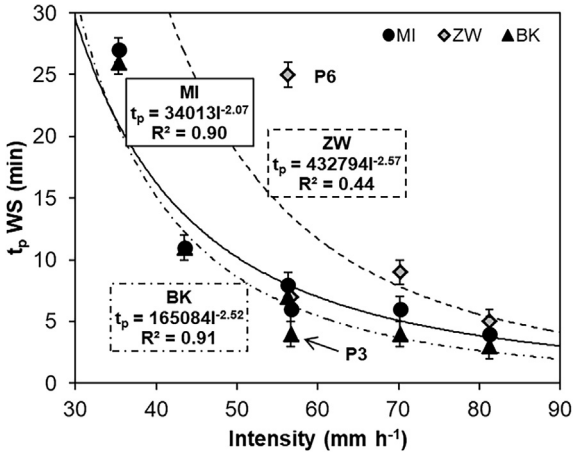

Fig. 9. Regression analysis of mean ponding time (t_pWS) for soil samples with wet-sealed (WS) surface initial condition and Mistelbach (MI), Zwerbach (ZW) and Býkovice (BK) soil, in correlation with rainfall intensity obtained under rainfall simulator at BAW. P3 and P6 show results obtained for positions 3 and 6 under rainfall simulator, respectively. Whiskers represent ± standard deviation of mean t_p within replicates (n = 3).

the intensity rates (Fig. 9). The results showed high agreement between t_p and rainfall intensity with R^2 of 0.90 and 0.91 obtained for MI and BK soil, respectively. The R^2 for ZW soil was remarkably lower, due to high difference in t_p between the positons 3 and 6, with same intensity rate of 56 mm h^{-1} (P3, P6 on Fig. 9). Larger drop diameter measured for position 3 (Table 3) could contribute to greater surface compaction during the previous simulation with AD initial condition. This eventually resulted in lower K_s for positon 3 and therefore, shorter t_p during the simulation with WS samples (Fig. 7-e). Similar results of t_p for position 3 and 6 were also observed for MI soil during the simulation with AD initial condition (Table 5).

4. Discussion

4.1. Effect of rainfall kinetic energy produced by two rainfall simulators on splash erosion

The results of splash erosion obtained from both rainfall simulators revealed comparable trend of splash development in relation with KE (Fig. 6). However, twice as high splash erosion rates were measured for the rainfall simulator at BOKU. The velocities of raindrops were crucial in defining rainfall kinetic energy, where higher velocities contributed to higher KE for BOKU rainfall simulator (Fig. 4-b). The differences in drop size-velocity distribution between different rainfall simulators can result in the significantly different splash erosion rates. This should be considered when comparing the splash erosion results from different studies.

The rainfall KE produced by rainfall simulator is often defined by (uniform) drops of different size and fall height, while the KE obtained in the field conditions depends primarily on drop size distribution (Van Dijk et al., 2003). Similar was observed with the two rainfall simulators used in present study. The drop distribution of rainfall simulator at the BAW was too uniform to describe the natural rainfall and the velocities of larger drops (> 1.3 mm) were far from the terminal velocity, defined by Atlas et al. (1973). On the contrary, the BOKU rainfall simulator produced higher velocities for most of drops in the same diameter class. However, large drops were still under the terminal velocity line (Fig. 5). Related to drop terminal velocity under the simulated rainfall, Iserloh et al. (2013) concluded that larger drops produced by different rainfall simulators are usually not able to reach their terminal velocity (mostly due to low fall height). For this reason, the rainfall KE produced in the laboratory cannot completely represent KE of natural rainfall.

4.2. Effect of soil water content and surface condition on splash erosion

Fluctuations in splash rates obtained from individual rainfall simulator were combined effect of θ_a and seal development affected by KE. Lower θ_a (AD initial condition) contributed to greater splash erosion for samples exposed to high intensities and KE. Therefore, splash erosion could be described as a linear or power function of increasing KE for AD initial condition, which was also obtained in previous studies (Fernández-Raga et al., 2010; Sharma et al., 1991; Zumr et al., 2019). However, appearance of surface ponding in the last stage of rainfall simulation indicated the reduction in soil infiltration rate, characterized by lower soil permeability due to surface seal formation (Assouline, 2004; Liu et al., 2011; Sharma et al., 1995). Surface seal was easily observable on the soil samples exposed to high intensities (> 50 mm h^{-1}) with completely smooth soil surface after the rainfall simulation. In addition, significantly lower K_s (Fig. 7) for the samples exposed to high intensities indicated the beginning of surface seal formation.

In the following rainfall simulation with WS soil samples splash erosion decreased with increased rainfall KE (Fig. 6-b,e,h). The final splash erosion rates for samples exposed to highest KE were evidently lower compared to rates for AD surface condition. According to results in Table 5, surface ponding was initiated earlier than for AD and DC initial condition. This was contributed to high θ_a, where early surface ponding at higher θ_a results from rapid decline in the hydraulic gradient for intensive rainfall in combination with a lower storage capacity (Liu et al., 2011; Vermang et al., 2009). Furthermore, partly formed seals (for MI and ZW soil) from previous simulation with AD soil samples probably resulted in higher resistance of soil surface to splash erosion prior to surface ponding. Following surface ponding eventually lowered the raindrop impact on soil surface preventing the further splash erosion (Poesen, 1981). Similar results were reported by Vermang et al. (2009), where soil detachment decreased along with surface seal development and formation of shallow water layer by surface runoff.

During the simulation with DC initial condition, the influence of the

θ_a on reduction in t_p could be excluded, since the initial θ_a was approximately three times lower. Therefore, the reduction in infiltration rates followed by surface ponding (Table 5) may be due to already developed seals, after previous exposure of the samples to rainfall (with AD and WS initial condition). Unlikely to splash erosion for WS initial condition, the reduction in splash erosion rates was noticed only for BK soil under the BOKU rainfall simulator (Fig. 6-i). Results for other soils, however, suggested the increase in splash erosion compared to samples with AD initial condition under lower rainfall intensities. Opposite results were reported by Le Bissonnais et al. (1995), where drying of aggregates increased the stability against aggregate breakdown. According to Lado et al. (2004), the wetting rate in combination with initial water content determined the magnitude of slaking forces causing aggregate break down. These forces are greater if the aggregates are drier. Therefore, it could be hypothesized that the higher splash erosion rates during the rainfall simulation with DC initial condition for the MI and ZW samples could be contributed to aggregate destruction by slaking.

Generally splash erosion increased or did not vary between the simulations on samples with different initial conditions which were not affected by surface ponding. This was related mostly to samples exposed to lower intensity and KE (< 660 J m^{-2} h^{-1}). High θ_a for WS samples may result in higher splash erosion (compared to AD initial condition) for the slow ponding soil samples considering both ZW and MI soil (Fig. 6-a-f). The findings of Beczek et al. (2019) and Gao et al. (2003) confirmed that the mass of monitored eroded material increased with higher θ_a due to lower cohesion between soil particles, considering that no surface seal was present.

Following the above lines discussed, it is difficult to select one factor that describes the differences in splash erosion rates for different initial conditions and soils. Soil conditions before rainfall and their variability during the rainfall will contribute to variation in splash characteristics. Depending on rainfall, soil structure, physico-chemical properties and θ_a, response of the soil to raindrop impact will vary. Nevertheless, for the three soils studied under rainfall conditions in this experiment can be concluded that reduction in splash erosion was primarily attributed to surface ponding initiated by high rainfall intensities and subsequent sealing formation. High initial θ_a reduced soil infiltration capacity and induced faster surface ponding (for WS initial condition) with decrease in splash erosion rates (Walker et al., 2007). In the case of the three soils studied here, initially lower K_s for MI and BK soil could be attributed to lower porosity considering lower clay content (12–18%) than for ZW soil, as indicated by Wei et al. (2015). Furthermore, it should be noted that beside the soil texture other soil properties, such as OC and calcium cations (Ca^{2+}) could affect the soil hydraulic properties (Wuddivira and Camps-Roach, 2007) and eventually splash erosion rates. However, we could not establish correlation between K_s and OC or $CaCO_3$ (contains Ca^{2+}) for the three soils presented here (Table 1, Fig. 7).

4.3. Effect of soil properties on surface seal formation

Soil detachment is depended on aggregate strength and after seal development on seal strength (Vermang et al., 2009). The both are highly related to soil physico-chemical properties (Mualem et al., 1990). Stability of aggregates obtained for three soils could not explain differences in the splash rates or the seal development in the present study. For example, BK soil had highest ratio of stable aggregates (Table 1), however, the splash erosion rates for AD surface condition did not significantly ($P < 0.05$) differ compared to MI soil with lowest AS. High OC and $CaCO_3$ content could be favourable for higher soil AS (Le Bissonnais et al., 1993). Similar OC content between the soils (Table 1) and low $CaCO_3$ soil could not explain higher AS for BK. However, it might be considered that higher clay content for MI and ZW soil could promote the slaking forces during the wet-sieving and decrease of the AS. Furthermore, the K_s obtained for BK was lowest compared to other two soils and did not vary between the simulations (Fig. 8-c, Fig. 7-g-i). On the one hand, this could indicate that the KE did not have major effect on the surface seal formation. On the other hand, stable surface seal formation could be initiated in early stage of rainfall simulation with AD soil samples. Therefore, further development (decrease) was not detected. In addition to that, the BK soil had visibly smaller aggregates compared to other two soils. For this reason, the lower KE was needed to destroy aggregates and to form crust. In the study by Fox et al. (2007), smaller fractions were more susceptible to surface crusting and splash erosion than the coarser fractions. Furthermore, lower surface roughness due to smaller aggregates might indicate smaller depressional storage, which induced earlier surface runoff (Truman and Bradford, 1990).

ZW soil showed lowest splash erosion rates and high K_s for AD surface condition compared to three soils. Le Bissonnais et al. (1995) reported that soils with high OC content have lowest erosion rate in AD conditions. Similar values of OC content were obtained for three soils (Table 1). Considering this, low splash erosion rates for ZW soil in AD condition were not contributed to OC content. However, according to Vermang et al. (2009) and Xiao et al. (2018) during the fast wetting period on dry surface, formation stable aggregates is affected by cementing effect of clay particles trough the surface water tension. This may be the reason for higher resistance of the ZW soil to soil erosion and seal development.

Manny studies provided the evidence that formation of sealing was characteristics of soils with high silt content (Cheng et al., 2008; Rodrigo Comino et al., 2017; Truman and Bradford, 1990). This could be also applied on results obtained in this study for MI soil, characterized by high silt content and low AS (Table 1). Assuming that the decrease in splash erosion and K_s was affected by surface seal formation, the MI soil showed highest reduction in K_s between the rainfall simulations among the three soils.

4.4. Effect of rainfall kinetic energy on surface seal formation

The obtained threshold values of KE required to form stable seal formation, confirmed the assumption of greater seal development under the soil surfaces exposed to higher KE. This was also stated by Bedaiwy (2008), where the important influence of KE on surface formation was highlighted. Constant or increasing splash erosion rates obtained for all three soils exposed to low intensity rates (< 35.3 mm h^{-1}) implied that accumulated KE throughout the simulations was lower than critical KE to initiate surface seal formation. However, high deviations between the replicates for K_s require more measurements in order to more precisely describe the process of surface crust development for certain scenarios.

5. Conclusion

In this study different scenarios of splash erosion development were obtained by applying simulated rainfall produced from two different rainfall simulators on soil samples with air-dried, wet-sealed and dry-crusted surface condition. Both rainfall simulators exhibited same trend of splash erosion development by applying similar range of intensities, though the total amount of splash rates where significantly different. This was contributed to differences in drop and velocity spectrum resulting in different kinetic energy produced for the same rainfall amount. Since splash erosion in primarily affected by raindrop impact, a special attention should be given when comparing the results obtained with different rainfall simulators due to variabilities in drop and velocity distribution.

The splash erosion rates increased with increasing kinetic energy for air-dried and dry-crusted soil samples with lower initial water content. Higher initial water content contributed to decrease (up to 70%) in splash erosion rates for the wet-sealed initial condition due to early surface ponding and sealing. Time to ponding measurements verified

that decrease in soil infiltration rate for wet-sealed condition is the function of increasing intensity with R^2 of 0.90 and 0.91 for silt loam and loamy sand soil, respectively. The formed seal layer can be reflected on decrease in saturated hydraulic conductivity, where the predominant factor for its reduction was kinetic energy. We identified a threshold rainfall kinetic energy from which stable surface seals are formed, which equals to 0.39 and 0.59 kJ m^{-2} h^{-1} for two silt loam soils used in this experiment. Considering high variability among replicates for saturated hydraulic conductivity measurements, it is difficult to identify clear relationship for some scenarios. Further experiments comparing more soil types should be conducted in order to precisely define soil specific properties controlling the splash erosion. In natural conditions soil is exposed to frequent changes in soil moisture and surface structure due to variable weather impacts. This research presents that the conditions before rainfall such as initial water content and surface condition highly affect soil erodibility, infiltration and final splash erosion. Therefore, including these parameters into soil erosion prediction models could significantly improve their accuracy.

Declaration of Competing Interest

The authors declare that they have no known competing financial interests or personal relationships that could have appeared to influence the work reported in this paper.

Acknowledgements

This research was performed within the project “Kinetic energy of rainfall as driving force of soil detachment and transport“, jointly funded by the Austrian Science Fund (FWF), grant number I 3049-N29 and the Czech Science Foundation (GACR), grant number GF17-33751L. The authors would like to thank to editors and anonymous reviewers for their useful comments and suggestions.

References

Armenise, E., Simmons, R.W., Ahn, S., Garbout, A., Doerr, S.H., Mooney, S.J., Sturrock, C.J., Ritz, K., 2018. Soil seal development under simulated rainfall: Structural, physical and hydrological dynamics. J. Hydrol. 556, 211–219. https://doi.org/10.1016/j.jhydrol.2017.10.073.

Assouline, S., 2004. Rainfall-induced soil surface sealing: a critical review of observations, conceptual models, and solutions. Vadose Zo. J. 3, 570–591. https://doi.org/10.2113/3.2.570.

ÖNORM L 1080, 2013. Chemische Bodenuntersuchungen – Bestimmung des organischen Kohlenstoffs durch trockene Verbrennung mit und ohne Berücksichtigung von Carbonaten. Austrian Standards, Vienna, Austria.

ÖNORM L 1050, 2016. Boden als Pflanzenstandort – Begriffsbestimmungen, Untersuchungsverfahren. Austrian Standards, Vienna, Austria.

Assouline, S., Mualem, Y., 2002. Infiltration during soil sealing: The effect of areal heterogeneity of soil hydraulic properties. Water Resour. Res. 38, 22-1-22–9. https://doi.org/10.1029/2001wr001168.

Assouline, S., Mualem, Y., 1997. Modeling the dynamics of seal formation and its effect on infiltration as related to soil and rainfall characteristics. Water Resour. Res. 33 (7), 1527–1536. https://doi.org/10.1029/96WR02674.

Atlas, D., Srivastava, R.C., Sekhon, R.S., 1973. Doppler radar characteristics of precipitation at vertical incidence. Rev. Geophys. 11, 1–35. https://doi.org/10.1029/RG011i001p00001.

Baumhardt, R.L., Römkens, M.J.M., Whisler, F.D., Parlange, J.-Y., 1990. Modeling infiltration into a sealing soil. Water Resour. Res. 26 (10), 2497–2505. https://doi.org/10.1029/WR026i010p02497.

Beczek, M., Ryżak, M., Sochan, A., Mazur, R., Bieganowski, A., 2019. The mass ratio of splashed particles during raindrop splash phenomenon on soil surface. Geoderma. https://doi.org/10.1016/j.geoderma.2019.03.028.

Bedaiwy, M.N.A., 2008. Mechanical and hydraulic resistance relations in crust-topped soils. Catena 72, 270–281. https://doi.org/10.1016/j.catena.2007.05.012.

Benjamini, Y., Hochberg, Y., 1995. Controlling the False Discovery Rate: A Practical and Powerful Approach to Multiple Testing. J. R. Stat. Soc. Ser. B. https://doi.org/10.1111/j.2517-6161.1995.tb02031.x.

Cheng, Q., Cai, Q., Ma, W., 2008. Comparative study on rain splash erosion of representative soils in China. Chin. Geogr. Sci. 18, 155–161. https://doi.org/10.1007/s11769-008-0155-9.

Dunn, J.O., 1964. Multiple comparison using rank sums. Technometrics.

Fernández-Raga, M., Campo, J., Rodrigo-Comino, J., Keesstra, S.D., 2019. Comparative analysis of splash erosion devices for rainfall simulation experiments: A laboratory study. Water (Switzerland) 11, 1–21. https://doi.org/10.3390/w11061228.

Fernández-Raga, M., Fraile, R., Keizer, J.J., Varela Teijeiro, M.E., Castro, A., Palencia, C., Calvo, A.I., Koenders, J., Da Costa Marques, R.L., 2010. The kinetic energy of rain measured with an optical disdrometer: An application to splash erosion. Atmos. Res. https://doi.org/10.1016/j.atmosres.2009.07.013.

Fernández-Raga, M., Palencia, C., Keesstra, S., Jordán, A., Fraile, R., Angulo-Martínez, M., Cerdà, A., 2017. Splash erosion: A review with unanswered questions. Earth-Sci. Rev. https://doi.org/10.1016/j.earscirev.2017.06.009.

Fox, D.M., Darboux, F., Carrega, P., 2007. Effects of fire-induced water repellency on soil aggregate stability, splash erosion, and saturated hydraulic conductivity for different size fractions. Hydrol. Process. https://doi.org/10.1002/hyp.6758.

Gao, B., Walter, M.T., Steenhuis, T.S., Parlange, J.Y., Nakano, K., Rose, C.W., Hogarth, W.L., 2003. Investigating ponding depth and soil detachability for a mechanistic erosion model using a simple experiment. J. Hydrol. 277, 116–124. https://doi.org/10.1016/S0022-1694(03)00085-4.

Ghadiri, H., Payne, D., 1977. Raindrop impact stress and the breakdown of soil crumbs. J. Soil Sci. https://doi.org/10.1111/j.1365-2389.1977.tb02233.x.

Guy, B.T., Dickinson, W.T., Rudra, R.P., 1987. Roles of rainfall and runoff in the sediment transport capacity of interrill flow. Trans. Am. Soc. Agric Eng. https://doi.org/10.13031/2013.30575.

Hairsine, P.B., Rose, C.W., 1991. Rainfall detachment and deposition: sediment transport in the absence of flow-driven processes. Soil Sci. Soc. Am. J. https://doi.org/10.2136/sssaj1991.03615995005500020003x.

Iserloh, T., Ries, J.B., Arnáez, J., Boix-Fayos, C., Butzen, V., Cerdà, A., Echeverría, M.T., ernández-Gálvez, J., Fister, W., Geißler, C., Gómez, J.A., Gómez-Macpherson, H., Kuhn, N.J., Lázaro, R., León, F.J., Martínez-Mena, M., Martínez-Murillo, J.F., Marzen, M., Mingorance, M.D., Ortigosa, L., Peters, P., Regüés, D., Ruiz-Sinoga, J.D., Scholten, T., Seeger, M., Solé-Benet, A., Wengel, R., Wirtz, S., 2013. European small portable rainfall simulators: A comparison of rainfall characteristics. Catena 110, 100–112. https://doi.org/10.1016/j.catena.2013.05.013.

IUSS Working Group WRB, 2014. World Reference Base for Soil Resources 2014. World Soil Resources Report. FAO, Rome.

Kemper, W.D., Koch, E.J., 1966. Aggregate stability of soils from western United States and Canada. United State Dep. Agric.

Kinnell, P.I.A., 2005. Raindrop-impact-induced erosion processes and prediction: A review. Hydrol. Process. 19, 2815–2844. https://doi.org/10.1002/hyp.5788.

Kinnell, P.I.A., 1982. Laboratory studies on the effect of drop size on splash erosion. J. Agric. Eng. Res. 27, 431–439. https://doi.org/10.1016/0021-8634(82)90081-6.

Klute, A., Dirksen, C., 1987. Hydraulic conductivity of Saturated soils. In: Klute, A. (Ed.), Methods of Soil Analysis, Part 1. Physical and Mineralogical Methods. American Society of Agronomy - Soil Science Socity of America, Madison, WI, pp. 694–700.

Kruskal, W.H., Wallis, W.A., 1952. Use of ranks in one-criterion variance analysis. J. Am. Stat. Assoc. https://doi.org/10.1080/01621459.1952.10483441.

Lado, M., Ben-Hur, M., Shainberg, I., 2004. Soil wetting and texture effects on aggregate stability, seal formation, and erosion. Soil Sci. Soc. Am. J. https://doi.org/10.2136/sssaj2004.1992.

Le Bissonnais, Y., 2016. Aggregate stability and assessment of soil crustability and erodibility: I. Theory and methodology. Eur. J. Soil Sci. 67, 11–21. https://doi.org/10.1111/ejss.4_12311.

Le Bissonnais, Y., Singer, M.J., Bradford, J.M., 1993. Assessment of soil erodibility: the relationship between soil properties, erosion processes and susceptibility to erosion. Farm L. Eros. Temp. plains Environ. hills. Proc. Symp. Saint-Cloud, Paris, 1992. https://doi.org/10.1016/b978-0-444-81466-1.50012-5.

Le Bissonnais, Y., Renaux, B., Delouche, H., 1995. Interactions between soil properties and moisture content in crust formation, runoff and interrill erosion from tilled loess soils. Catena 25, 33–46. https://doi.org/10.1016/0341-8162(94)00040-L.

Liu, H., Lei, T.W., Zhao, J., Yuan, C.P., Fan, Y.T., Qu, L.Q., 2011. Effects of rainfall intensity and antecedent soil water content on soil infiltrability under rainfall conditions using the run off-on-out method. J. Hydrol. 396, 24–32. https://doi.org/10.1016/j.jhydrol.2010.10.028.

McIntyre, D.S., 1958. Soil splash and the formation of surface crusts by raindrop impact. Soil Sci. https://doi.org/10.1097/00010694-195805000-00005.

Morgan, R.P.C., 2005. Soil Erosion and Conservation, third ed. Blackwell Publishing company, Oxford.

Morgan, R.P.C., 1981. Field measurement of splash erosion. Int. Assoc. Sci. Hydrol. Publ. 133, 373–382.

Mualem, Y., Assouline, S., Rohdenburg, H., 1990. Rainfall induced soil seal (A) A critical review of observations and models. Catena. https://doi.org/10.1016/0341-8162(90)90008-2.

ÖNORM L 1084, 2016. Chemische Bodenuntersuchungen - Bestimmung von Carbonat unter Berücksichtigung von Luftdruck und Temperatur. Austrian Standards, Vienna, Austria.

ÖNORM L1061-1, 2002. Physikalische Bodenuntersuchungen – Bestimmung der Korngrößenverteilung des Mineralbodens; Teil 1: Grobboden. Austrian Standards, Vienna, Austria.

ÖNORM L1061-2, 2002. Physikalische Bodenuntersuchungen – Bestimmung der Korngrößenverteilung des Mineralbodens; Teil 2: Feinboden. Austrian Standards, Vienna, Austria.

ÖNORM L 1086-1, 2014. Chemische Bodenuntersuchungen - Extraktion der effektiv austauschbaren Kationen Ca++, K+, Mg++, Na+ sowie Al+++, Fe+++, Mn++ und H+ mit Bariumchlorid-Lösung und Ermittlung der Austauschkapazität. Wien.

OTT, 2005. Operating instructions. Present weather sensor Parsivel. Kempten.

Poesen, J., 1981. Rainwash experiments on the erodibility of loose sediments. Earth Surf. Process. Landforms. https://doi.org/10.1002/esp.3290060309.

Quansah, C., 1981. The effect of soil type, slope, rain intensity and their interactions on

splash detachment and transport. J. Soil Sci. https://doi.org/10.1111/j.1365-2389.1981.tb01701.x.
R Development Core Team, 2015. R: A language and environment for statistical computing. R Foundation for Statistical Computing, Vienna, Austria. URL http://www.R-project.org/. R Found. Stat. Comput. Vienna, Austria. https://doi.org/10.1007/978-3-540-74686-7.
Rodrigo Comino, J., Senciales, J.M., Ramos, M.C., Martínez-Casasnovas, J.A., Lasanta, T., Brevik, E.C., Ries, J.B., Ruiz Sinoga, J.D., 2017. Understanding soil erosion processes in Mediterranean sloping vineyards (Montes de Málaga, Spain). Geoderma 296. https://doi.org/10.1016/j.geoderma.2017.02.021.
Rose, C.W., 1960. Soil detachment caused by rainfall. Soil Sci. 89, 28–35. https://doi.org/10.1097/00010694-196001000-00005.
Salles, C., Poesen, J., 2000. Rain properties controlling soil splash detachment. Hydrol. Process. 14, 271–282. https://doi.org/10.1002/(SICI)1099-1085(20000215)14:2<271::AID-HYP925>3.0.CO;2-J.
Salles, C., Poesen, J., Govers, G., 2001. A comparison of rain erosivity parameters for predicting soil detachment on interrills. Sustain. Glob. Farm, 10th Int. Soil Conserv. Organ. Meet. My 24–29, 1999 834–837.
Sharma, P.P., Gupta, S.C., Foster, G.R., 1995. Raindrop-induced soil detachment and sediment transport from interrill areas. Soil Sci. Soc. Am. J. 59, 727. https://doi.org/10.2136/sssaj1995.03615995005900030014x.
Sharma, P.P., Gupta, S.C., Rawls, W.J., 1991. Soil detachment by single raindrops of varying kinetic energy. Soil Sci. Soc. Am. J. 55, 301. https://doi.org/10.2136/sssaj1991.03615995005500020001x.
Strauss, P., Pitty, J., Pfeffer, M., Mentler, A., 2000. Rainfall simulation for outdoor experiments. Curr. Res. methods to assess Environ. fate Pestic. 329–333.
Truman, C.C., Bradford, J.M., 1990. Effect of antecendet soil moisture on splash detachment under simulated rainfall.
Van Dijk, A.I.J.M., Bruijnzeel, L.A., Eisma, E.H., 2003. A methodology to study rain splash and wash processes under natural rainfall. Hydrol. Process. 17, 153–167. https://doi.org/10.1002/hyp.1154.
Vermang, J., Demeyer, V., Cornelis, W.M., Gabriels, D., 2009. Aggregate stability and erosion response to antecedent water content of a loess soil. Soil Sci. Soc. Am. J. 73, 718. https://doi.org/10.2136/sssaj2007.0134.
Walker, J.D., Walter, M.T., Parlange, J.Y., Rose, C.W., van Meerveld, H.J.T., Gao, B., Cohen, A.M., 2007. Reduced raindrop-impact driven soil erosion by infiltration. J. Hydrol. 342, 331–335. https://doi.org/10.1016/j.jhydrol.2007.06.003.
Wei, Y., Wu, X., Cai, C., 2015. Splash erosion of clay-sand mixtures and its relationship with soil physical properties: The effects of particle size distribution on soil structure. Catena 135, 254–262. https://doi.org/10.1016/j.catena.2015.08.003.
Wischmeier, W., Smith, D., 1978. Predicting rainfall erosion losses: a guide to conservation planning, U.S. Department of Agriculture Handbook No. 537. https://doi.org/10.1029/TR039i002p00285.
Wischmeier, W.H., Johnson, C.B., Cross, B.V., 1971. Soil erodibility nomograph for farmland and construction sites. J. Soil Water Conserv.
Wuddivira, M.N., Camps-Roach, G., 2007. Effects of organic matter and calcium on soil structural stability. Eur. J. Soil Sci. 58, 722–727. https://doi.org/10.1111/j.1365-2389.2006.00861.x.
Xiao, H., Liu, G., Zhang, Q., Fenli, Z., Zhang, X., Liu, P., Zhang, J., Hu, F., Elbasit, M.A.M.A., 2018. Quantifying contributions of slaking and mechanical breakdown of soil aggregates to splash erosion for different soils from the Loess plateau of China. Soil Tillage Res. 178, 150–158. https://doi.org/10.1016/j.still.2017.12.026.
Zumr, D., Mützenberg, D.V., Neumann, M., Jeřábek, J., Laburda, T., Kavka, P., Johannsen, L.L., Zambon, N., Klik, A., Strauss, P., Dostál, T., 2019. Experimental setup for splash erosion monitoring—study of silty loam splash characteristics. Sustainability 12, 157. https://doi.org/10.3390/su12010157.